The Regulatory RNAs of Bacillus subtilis

Mars, Ruben

Chapter 5

Small Regulatory RNA-Induced Growth Rate Heterogeneity of *Bacillus subtilis*

Ruben A. T. Mars, Pierre Nicolas, Mariano Ciccolini, Ewoud Reilman, Alexander Reder, Marc Schaffer, Ulrike Mäder, Uwe Völker, Jan Maarten van Dijl, and Emma L. Denham

In revision

Abstract

Isogenic bacterial populations can consist of cells displaying heterogeneous physiological traits. Small-regulatory RNAs (srRNAs) could affect this heterogeneity since they act by fine-tuning mRNA or protein levels to coordinate the appropriate cellular behavior. Here we show that the srRNA RnaC/S1022 from the Gram-positive bacterium *Bacillus subtilis* can suppress exponential growth by modulation of the transcriptional regulator AbrB. Specifically, the post-transcriptional *abrB*-RnaC/S1022 interaction allows *B. subtilis* to increase the cell-to-cell variation in AbrB protein levels, despite strong negative autoregulation of the *abrB* promoter. This behavior is consistent with existing mathematical models of srRNA action, thus suggesting that induction of protein expression noise could be a new general aspect of srRNA regulation. Importantly, we show that the srRNA-induced diversity in AbrB levels generates heterogeneity in growth rates during the exponential growth phase. Based on these findings, we hypothesize that the resulting subpopulations of fast- and slow-growing *B. subtilis* cells reflect an evolutionary conserved bet-hedging strategy for enhanced survival of unfavorable conditions.

Introduction

In their natural habitat, bacteria constantly adapt to changing environments while simultaneously anticipating further disturbances. To efficiently cope with these changes, intricate interlinked metabolic and genetic regulation has evolved (1). This complex regulatory network includes the action of small regulatory RNAs (srRNAs) (2). srRNAs are a widespread means for bacterial cells to coordinate (stress) responses by fine-tuning levels of mRNAs or proteins, and they have been studied in great detail in Gram-negative bacteria (3). Regulation by srRNAs takes place by short complementary base pairing to their target mRNA molecules, for instance in the region of the ribosome-binding site (RBS) to inhibit translation or trigger mRNA degradation. In Gram-negative bacteria these srRNA-mRNA interactions are mediated by the RNA chaperone Hfq (4). However, the Hfq homologue in the Gram-positive model bacterium *Bacillus subtilis* has no effect on the regulation of the eight srRNA targets reported in this species so far (5, 6, 7). Owing to the complexity of srRNA regulation, only a relatively small number of studies have focused specifically on the physiological necessity of srRNA-target interactions. This is again particularly true for Gram-positive bacteria, such as *B. subtilis*, despite the fact that many potential srRNAs have been identified (8, 9).

Within a bacterial population, genes and proteins can be expressed with a large variability, with high expression levels in some cells and low expression levels in others (10). Examples of expression heterogeneity in *B. subtilis* are the extensively studied development of natural competence for DNA binding and uptake and the differentiation into spores (11, 12, 13). In both cases, expression heterogeneity is generated by positive feedback loops, and results in bistable or ON-OFF expression of crucial regulators (14). Distinctly from bistabilty, proteins can also be expressed with large cell-to-cell variability. This variation in expression levels, or noise, can originate from intrinsic or extrinsic sources (15, 16). Extrinsic noise is related to cell-to-cell fluctuations in numbers of RNA polymerase, numbers of genome copies, or numbers of free ribosomes. Conversely, intrinsic noise is caused by factors directly involved in the transcription or translation of the respective gene or protein. Interestingly, particularly noisy genes are often found to be regulators of development and bacterial persistence (12, 17, 18). Because of the importance of noise in protein expression, cells have evolved mechanisms to regulate the noise levels of at least some proteins (10). Reducing noise levels has been suggested as an important explanation why many transcriptional regulators in bacteria (40% in *E. coli* (19)) autorepress the transcription of their own promoter (i.e. negative autoregulation (NAR)).

AbrB is a global transcriptional regulator in Gram-positive bacteria, including the important human pathogens *Bacillus anthracis* and *Listeria monocytogenes* (20, 21). *B. subtilis* AbrB positively regulates some genes when carbon catabolite repression (CCR) is relieved (22), and negatively regulates the expression of over two hundred genes in the exponential growth phase (23). Transcription of *abrB* is negatively autoregulated by binding of AbrB tetramers to the *abrB* promoter (24, 25). Upon entry into stationary phase, *abrB* transcription is repressed via increasing levels of Spo0A-P and AbrB is inactivated by AbbA (26, 27). The resulting AbrB depletion is consequently followed by activation of AbrB repressed genes, which are often important for stationary phase processes. Notably, because of its role in the elaborate sporulation and competence decision making network (26, 27), AbrB has mainly been studied in the context of entry into stationary phase while much less is known about its exact role in the exponential growth phase.

We selected putative srRNAs from a rich tiling array dataset of 1583 non-coding RNAs (ncRNAs) (9). This selection was made for evolutionary conserved putative srRNAs with a high expression level on defined minimal medium. Deletion strains of these putative *B. subtilis* srRNAs were subsequently tested for growth phenotypes. One srRNA - RnaC/S1022 - stood out since the mutant strain displayed a strongly increased final optical density on minimal medium with

sucrose as the sole carbon source. The present study was therefore aimed at determining how RnaC/S1022 influences the growth of *B. subtilis*. Inspection of evolutionary conserved predicted RnaC/S1022 targets indicated that the aberrant growth phenotype could relate to elevated AbrB levels. Here we show that, under certain conditions, *B. subtilis* employs RnaC/S1022 to post-transcriptionally modulate AbrB protein expression noise. The observed noise in AbrB protein levels is remarkable, because the *abrB* gene displays low transcriptional noise consistent with its NAR. Importantly, the srRNA-induced noise in the AbrB protein levels generates growth rate heterogeneity in the exponential phase.

Results

RnaC/S1022 deletion enhances growth on minimal medium

RnaC/S1022 was first identified in a systematic screening of *B. subtilis* intergenic regions with an oligonucleotide microarray (28). RnaC/S1022 is located in between *yrhK*, a gene of unknown function, and *cypB*, encoding cytochrome P450 NADPH-cytochrome P450 reductase (also known as *yrhJ*). We tested the conservation of the *B. subtilis* RnaC/S1022 sequence with BLAST analysis against a set of 62 *Bacillus* genomes, and found evolutionary conservation in a clade of the phylogenetic tree consisting of *B. subtilis* sp., *B. atrophaeus*, and *B. amyloliquefaciens* (Figure 1A). Within these 19 genomes, the 5' and 3' ends of the RnaC/S1022 sequence are conserved, but the core sequence is disrupted in all 9 *B. amyloliquefaciens* genomes. An alignment of RnaC/S1022 from the remaining 10 genomes was used to predict its secondary structure using the locARNA tool (29) (Figure 1B). This analysis predicts RnaC/S1022 to fold into a stable structure (Gibbs free energy -38.5 kcal/mol for *B. subtilis*).

RnaC/S1022 was recently included in a screen for possible functions of conserved putative srRNAs identified by Nicolas et al. (9) that are highly expressed on M9 minimal medium supplemented with different carbon sources (data not shown). Here, the RnaC/S1022 mutant stood out, because it consistently grew to a higher optical density (OD) in M9 minimal medium supplemented with sucrose (M9S) than the parental strain (Figure 1C). This effect was less pronounced in M9 with glucose (M9G). Since transcription of RnaC/S1022 is exclusively regulated by SigD (28), we also tested a *sigD* mutant for growth under these conditions. Interestingly, the Δ*sigD* mutant displayed similar growth characteristics as the ΔRnaC/S1022 mutant. Differential growth and increased competitiveness was previously reported for a *sigD* mutant (30), and our observations suggest that in some conditions the increased final OD of Δ*sigD* is partly due to deregulation of RnaC/S1022.

AbrB *is a conserved predicted target of RnaC/S1022*

We wondered whether deregulation of an srRNA target was responsible for the remarkable growth phenotype observed for the ΔRnaC/S1022 mutant and decided to perform exploratory target predictions using TargetRNA (31). Predicting srRNA targets can be successful, but target verification is complicated by the large number of false-positively predicted targets. We argued that additional information about the likelihood of a true target could be obtained by determining whether the predicted interaction is conserved over evolutionary time. To identify predicted RnaC/S1022-target interactions that are conserved, a bioinformatics pipeline was established that predicts srRNA targets in genomes in which the RnaC/S1022 sequence is conserved. Since we were interested in finding true *B. subtilis* srRNA targets, we only considered targets also predicted in *B. subtilis*, and these are listed in Supplemental Table I. This analysis reduced the number of considered RnaC/S1022 targets to 47 (from 147 predicted targets for TargetRNA_v1 predictions with P value ≤ 0.01 on the *B. subtilis* 168 genome). In this conserved predicted target list, the presence of seven sporulation-related genes is remarkable (*phrA*, *spoVAD*,

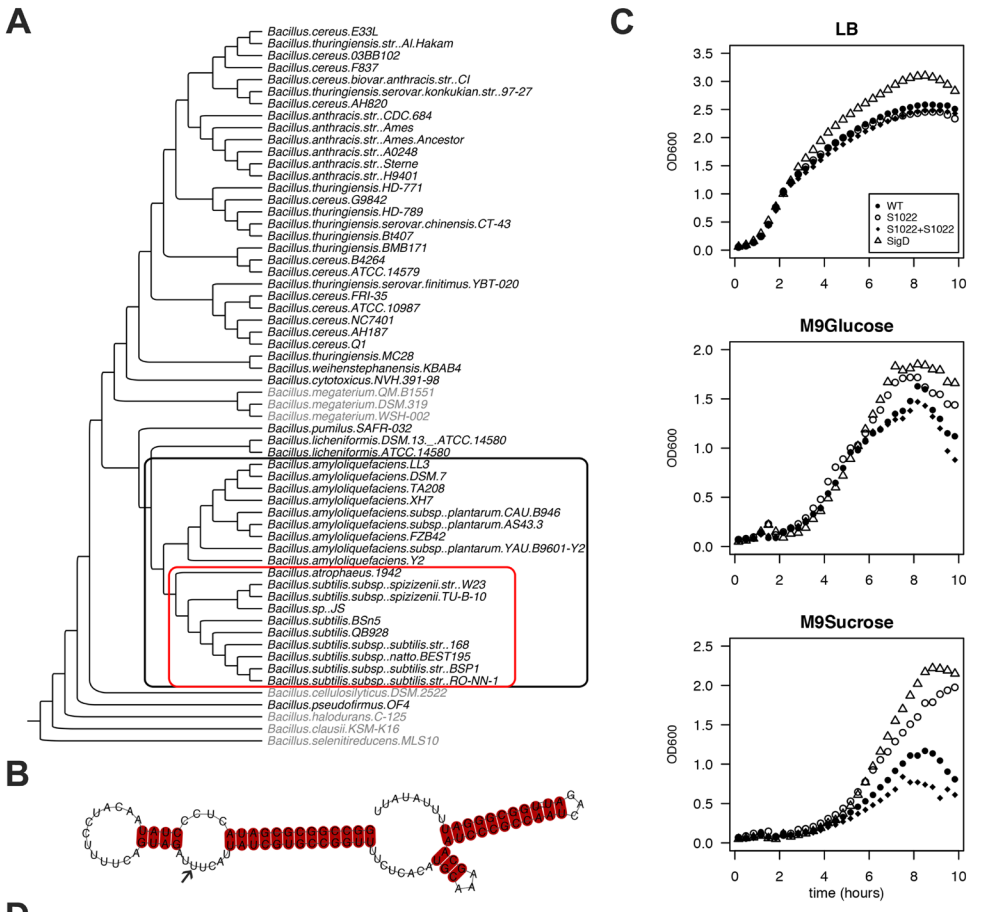

D

Species	Start	Stop	Indentity	Rank	P value	srRNA start	srRNA stop	mRNA start	mRNA stop
Bacillus_JS_uid162189	4	123	0.99	79	0.01	48	79	-16	13
Bacillus_subtilis_168_uid57675	1	126	1.00	98	0.01	51	82	-10	19
Bacillus_subtilis_BSn5_uid62463	1	123	0.98	83	0.01	51	82	-16	13
Bacillus_subtilis_BSP1_uid184010	4	126	1.00	83	0.01	48	79	-10	19
Bacillus_subtilis_natto_BEST195_uid183001	1	126	1.00	95	0.01	51	82	-16	13
Bacillus_subtilis_QB928_uid173926	1	126	1.00	93	0.01	51	82	-10	19
Bacillus_subtilis_RO_NN_1_uid158879	4	126	0.99	81	0.01	48	79	-16	13
Bacillus_atrophaeus_1942_uid59887	11	78	0.89	48	0.01	43	61	-6	15
Bacillus_subtilis_spizizenii_TU_B_10_uid73967	4	105	0.97	182	0.02	48	60	1	13
Bacillus_subtilis_spizizenii_W23_uid51879	4	123	0.94	166	0.01	48	60	1	13

Figure 1. The RnaC/S1022 growth phenotype is linked to the evolutionary target prediction of *abrB*.
A) Phylogenetic tree of *Bacillus* genomes. The tree was constructed based on an alignment of *rpoB* (present in 60 of the 62 genomes; except for two *Bacillus coagulans* genomes). The outer (black) box indicates genomes in which RnaC/S1022 is present. Inner (red) box indicates genomes in which the predicted RnaC/S1022-*abrB* interaction is conserved. A significant nBLAST hit for AbrB was not obtained for the species shaded in grey. B) LocARNA structural conservation alignment of RnaC/S1022 based on genomes in which the RnaC/S1022-*abrB* interaction is conserved. The arrow highlights the uracil base that is required for the interaction with *abrB*. C) Growth curves of parental strain 168^{trp+}, ΔRnaC/S1022, Δ*sigD*, and the ΔRnaC/S1022 pRMC-RnaC/S1022 complemented strain grown on LB, M9G or M9S. The experiment was repeated a minimum of three times in 96-well plates and shake flasks. Averages from triplicates from a representative 96-well plate experiment are shown. GFP and OD_{600} were monitored every 10 min. One in two time-points were plotted. D) Overview of the RnaC/S1022-*abrB* conserved predicted target interaction. Columns "Start" and "Stop" indicate the conserved RnaC/S1022 region, "Identity" the identify of this conserved region, "Rank" the ranking of the *abrB* target in all predicted RnaC/S1022 targets for this species. "P value" TargetRNA_v1 prediction P-value.

spoIIM, *spoIIIAG*, *cotO*, *sspG*, *spsI*). The sigma factor *sigM* was also conserved but, since a *sigM* mutant strain does not display a growth phenotype, this seemed unrelated to the observed growth phenotype of the ΔRnaC/S1022 mutant. In addition, two conserved predicted targets are involved in cell division (*racA* and *ftsW*), but we observed no cell-division abnormalities by live-imaging microscopy. Furthermore, the TCA cycle genes *citB* and *citZ* were predicted and tested by Western blot analysis, but no deregulation was observed (data not shown). The last conserved predicted target of initial interest was the transition state regulator *abrB* (Figure 1D). Reviewing the literature on *abrB* pointed us to an interesting observation where a *spo0A* mutant was reported to display increased growth rates on media similar to our M9 medium (22). Furthermore, it had been reported that AbrB has an additional role in modulating the expression of some genes during slow growth in suboptimal environments (32), which we argued could also be relevant to the M9S growth condition. Since *abrB* is a conserved predicted target of RnaC/S1022 (Figure 1D), we checked whether the presence of this srRNA coincides with the presence of the *abrB* gene. Indeed, *abrB* is conserved in 53 out of 62 available *Bacillus* genomes, and RnaC/S1022 is present in 19 of these 53 genomes. Accordingly, we hypothesized that RnaC/S1022 might be a regulator of AbrB.

AbrB levels are elevated in an RnaC/S1022 mutant

The combined clues from bioinformatics analyses and literature suggested that the growth phenotype of the ΔRnaC/S1022 mutant could relate to elevated AbrB levels. To test whether AbrB levels are indeed altered in this mutant, we performed Western blot and Northern blot analyses. This indeed revealed higher AbrB protein and mRNA levels in the RnaC/S1022 mutant (Figure 2). Importantly, the growth phenotype as well as AbrB protein and mRNA levels returned to wt by ectopic expression of RnaC/S1022 under control of its native promoter from the *amyE* locus (Figure 1C, Figure 2). We also tested the effects of a Δ*spo0A* mutation by Western and Northern blot analyses. Interestingly, the combined deletion of RnaC/S1022 and *spoOA* led to a further increase in the AbrB protein and mRNA levels compared to the already elevated levels in the *spo0A* mutant background. In addition, the increase in AbrB levels in cells grown on different growth media seemed to follow an increased expression of RnaC/S1022 (Figure 2). Lastly, we observed a three-fold reduced natural competence of the ΔRnaC/S1022 mutant, which is expected when the AbrB levels are elevated (33) (Supplemental Figure 1).

To test whether the AbrB levels were directly dependent on RnaC/S1022 levels, we placed the RnaC/S1022 complementation cassette in the *amyE* locus of the parental strain and used Western and Northern blotting to measure AbrB protein and mRNA levels. These analyses showed that both the AbrB protein and mRNA levels were further decreased, which is consistent with elevated RnaC/S1022 expression and increased *abrB* regulation (Figure 2). The amount of AbrB correlated well with the amount of RnaC/S1022, suggesting a stoichiometric relationship between these two molecules.

The RnaC/S1022 srRNA regulates AbrB *by a direct srRNA-mRNA interaction*

The observed stoichiometric relationship between AbrB and the srRNA RnaC/S1022 is suggestive of a direct srRNA – target interaction. The predicted interaction region in *B. subtilis* 168 spans a region from the RBS of *abrB* (-10) until 19 bp after the start of the *abrB* ORF of which the strongest consecutive stretch of predicted base-pair interactions are present from +7 bp till +19 bp (left top panel in Figure 3). In addition, only this region within the *abrB* coding sequence is part of the conserved predicted interaction region in *B. atrophaeus* and *B. subtilis spizinenzii* (Figure 1D). It has been reported that loop-exposed bases of srRNAs are more often responsible for regulation than bases in stems (34). Two loop regions in RnaC/S1022 are complementary

with the predicted *abrB* interaction region (one of two basepairs and one of seven basepairs) (Figures 1B and 3). We therefore decided to introduce a point-mutation by a U to A substitution in the middle of the 7 bp loop of RnaC/S1022 encoded by plasmid pRM3 and a compensatory mutation in a plasmid pRM15-borne truncated *abrB-gfp* reporter construct ($abrB_{trunc}$*-gfp*). Strains containing different combinations of the respective plasmids were grown on M9G and assayed by Flow Cytometry (FC) in the exponential growth phase. Cells containing one of the $abrB_{trunc}$*-gfp* constructs in combination with the empty pRM3 plasmid displayed a unimodal distribution in GFP levels (Fig. 3, lower panels). However, when the wt $abrB_{trunc}$*-gfp* was assayed in combination with the wt RnaC/S1022, a bimodal distribution in $AbrB_{trunc}$-GFP levels was observed (Fig. 3, top left). Interestingly, a unimodal fluorescence distribution was found when the wt $abrB_{trunc}$*-gfp* construct was combined with point-mutated RnaC/S1022* (Fig. 3, middle left) or the mutated $abrB^{*}_{trunc}$*-gfp* with the wt RnaC/S1022 (Fig. 3, top right). In the case of the point-mutated *abrB**-*gfp* construct, however, a bimodal fluorescence distribution was only observed when this construct was combined with the mutated RnaC/S1022* (Figure 3, middle right). This implies that a direct mRNA-srRNA interaction takes place between *abrB* and RnaC/S1022. Consistent with previous studies on other srRNA targets of *B. subtilis* (5, 6, 7), the direct RnaC/S1022-*abrB* regulation was not dependent on the presence of the Hfq homologue YmaH (data not shown).

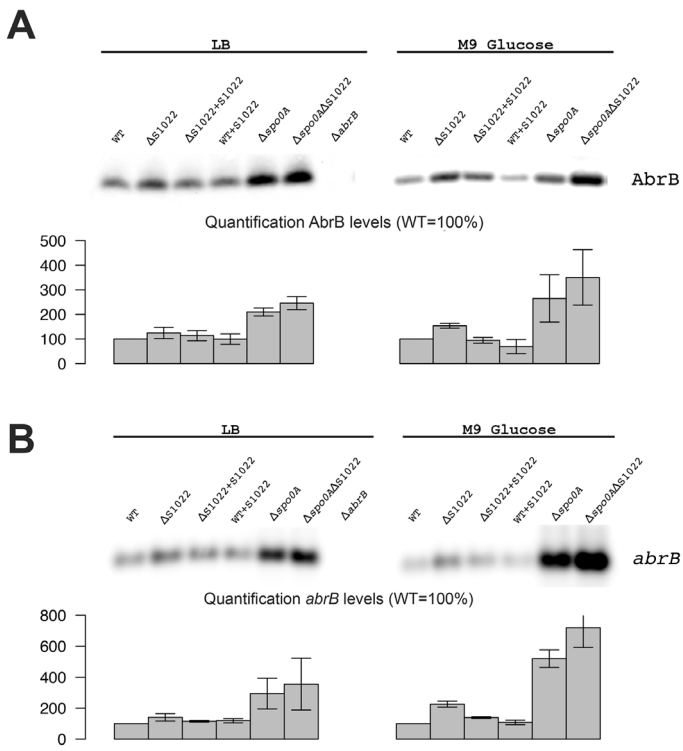

Figure 2. AbrB levels are dependent on the presence of RnaC/S1022.
A) AbrB Western blot analysis corrected with the internal control BdbD (only quantification shown). The effect of RnaC/S1022 absence is more pronounced on M9G which corresponds to a higher expression level in this growth condition. B) *abrB* Northern blot analysis on equal RNA amounts per lane. Quantifications are based on two independent experiments for Northern and three independent experiments for Western blots. Error bars represent the standard deviation. Data for M9S is not shown but is highly similar, be it more variable, to the M9G condition.

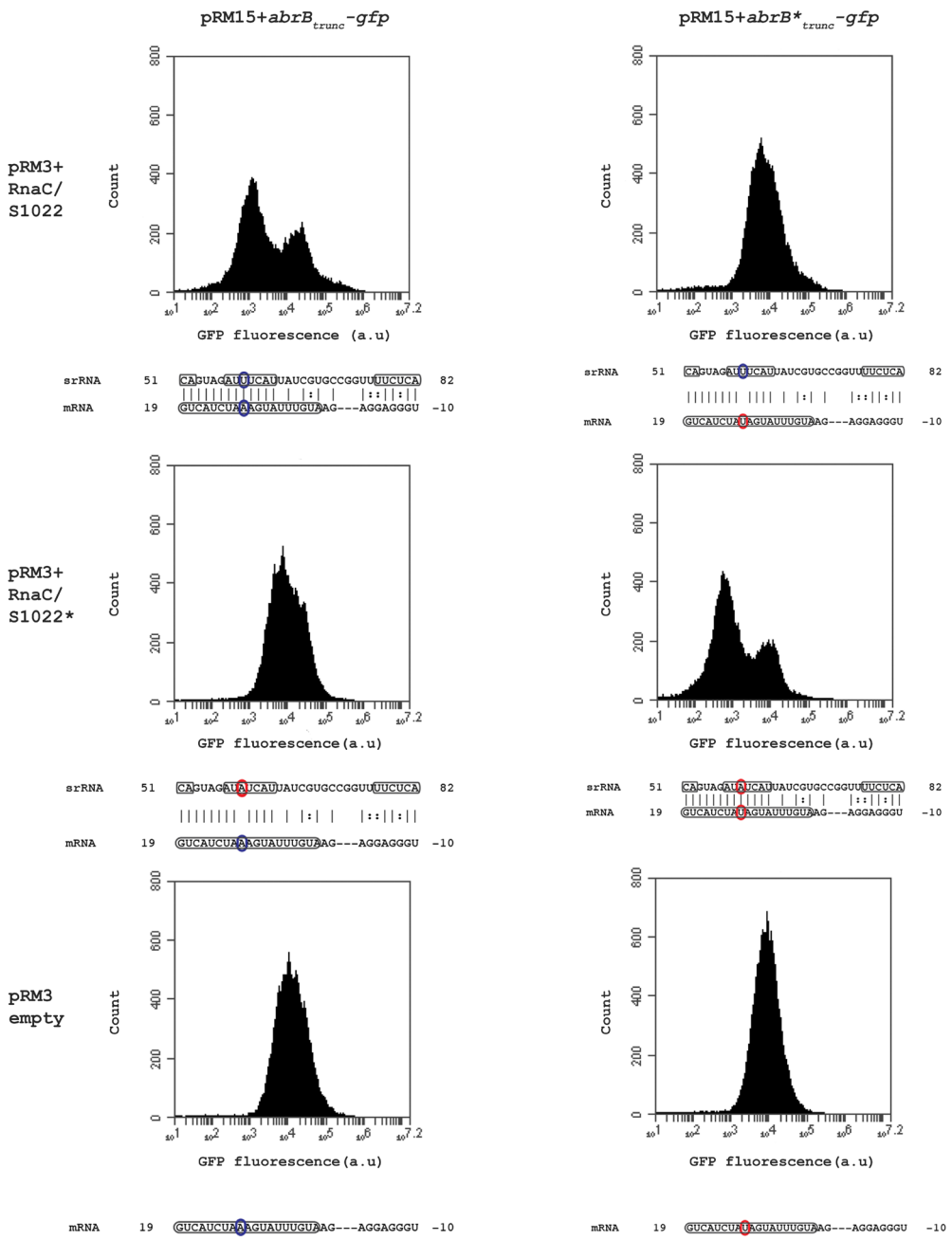

Figure 3. RnaC/S1022 regulates *abrB* by a direct mRNA-srRNA interaction.
Wt and base pair-substituted (marked with asterix *) *abrB*$_{trunc}$-*gfp* constructs were expressed from plasmid pRM15 and combined with one of three variants of the pRM3 plasmid (pRM3+RnaC/S1022, pRM3+RnaC/S1022*, pRM3 empty). All combinations of these constructs were assayed by FC and one representative histogram per combination is shown. Highlighted base-pairs in identical color indicate the presence of regulation, while highlighted base-pairs in two different colors indicate the absence of regulation. Boxed regions around the mRNA (*abrB*) indicate the coding sequence and for the srRNA (RnaC/S1022) boxes indicate the predicted exposed bases in the structure (from Figure 1B). The base pair found essential for srRNA regulation is present in a RnaC/S1022 loop region (RnaC/S1022*T58A) and is the 11th base in the coding region (*abrB**A11T).

RnaC/S1022 srRNA is condition-dependently expressed

Studying the condition-dependency of srRNA expression can give clues to its function and targets. To obtain high-resolution expression profiles, we constructed an integrative promoter fusion of RnaC/S1022 (35) and used this in a Live Cell Array approach. $P_{RnaC/S1022}$-*gfp* activity was compared with that of another SigD-dependent promoter, P_{hag}, which drives flagellin expression. We first verified that both fusions are not fluorescent when combined with a *sigD* mutation (Figure 4, D and E). These promoter fusion strains revealed that the expression of *hag* was consistently ~4 fold higher than that of RnaC/S1022 (Figure 4), which is in agreement with previously published expression data (9). On LB medium, the expression of both RnaC/S1022 and *hag* peaked in the late exponential and transition phase, while on both tested minimal media the peak in expression occurred in early exponential phase (Figure 4). This higher RnaC/S1022 expression level in the exponential phase on M9 relative to that in LB is in concordance with the stronger effect of ΔRnaC/S1022 on AbrB levels, as indicated by the Northern and Western blot analyses.

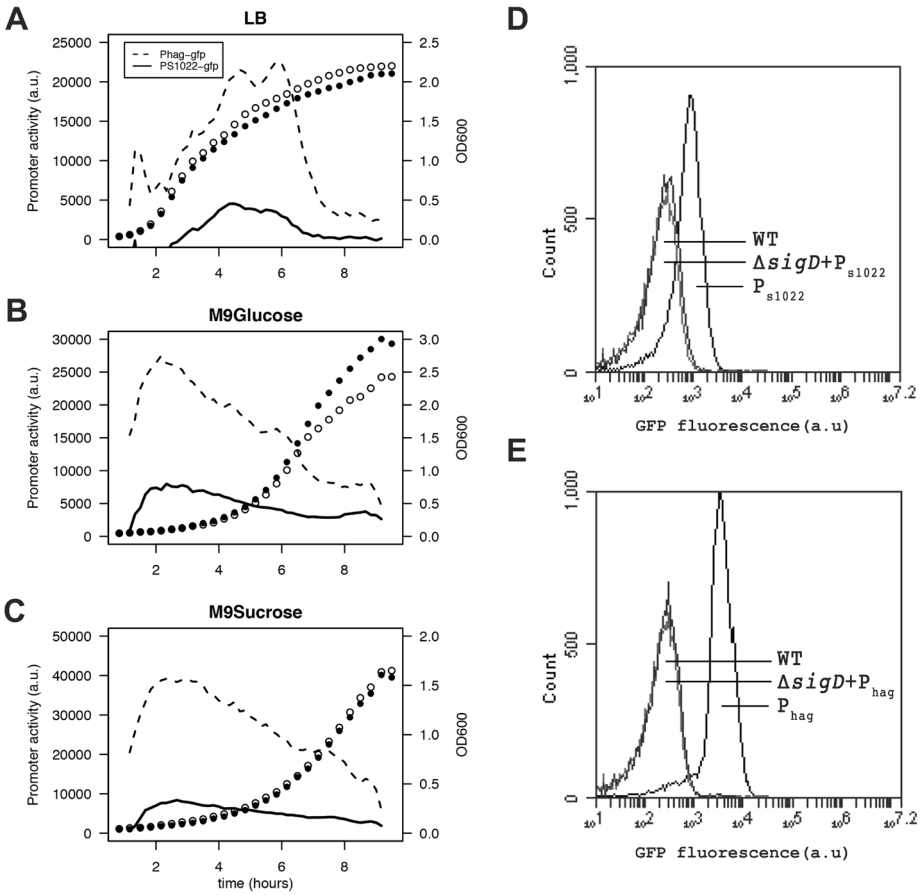

Figure 4. RnaC/S1022 is condition-dependently expressed.
Promoter activity of $P_{RnaC/S1022}$-*gfp* and P_{hag}-*gfp* in cells grown on LB (A), M9G (B), and M9S (C). Promoter activities were computed by subtraction of GFP level from the previous time-point. The experiment was done three times in triplicate. Average data from triplicate measurements of one representative experiment are shown. One in two time-points were plotted for the growth curve. D) Representative FC results for $P_{RnaC/S1022}$-*gfp* on mid-exponentially growing cells in M9G. E) same as in D for P_{hag}-*gfp*.

RnaC/S1022 srRNA modulates protein expression noise of AbrB-GFP

Experimental methods that measure average protein levels in a population obscure possible cell-to-cell variation. To further study the cell-to-cell variation of AbrB-GFP in the exponential growth phase (as observed in Figure 3), we therefore employed a chromosomally integrated full-length translational *abrB-gfp*mut3 fusion. In this AbrB-GFP strain all AbrB monomers have a C-terminally attached GFP molecule. While AbrB-GFP still localized to the nucleoid, this AbrB-GFP strain displayed somewhat reduced growth rates on media where AbrB is required for rapid growth (data not shown). Since the translational *abrB-gfp* fusion is chromosomally integrated at the *abrB* locus, this system is insensitive to fluctuations in noise levels by plasmid copy number variation and its chromosomal location in the division cycle.

We analyzed all AbrB-GFP strains by FC in the exponential phase on both LB and M9G. Noise measurements were not performed on M9S because of the strong growth difference between the parental and ΔRnaC/S1022 strain on this medium (Figure 1C). We observed that the difference between cells expressing AbrB-GFP at the highest level and those at the lowest level was large (Figure 5A). This means that AbrB-GFP is expressed with high noise (quantified as the coefficient of variation; CV%). Interestingly, we observed lower AbrB-GFP noise in strains lacking RnaC/S1022 and, crucially, the presence of an additional genomic RnaC/S1022 copy further increased AbrB-GFP noise. Remarkably, increased RnaC/S1022 levels only reduced the minimal expression level of the distribution while not affecting the maximum AbrB-GFP expression level (Figure 5A). There was a statistically significant positive linear correlation between RnaC/S1022 levels (0, 1 or 2 genomic copies) and AbrB-GFP noise (on LB for pooled data points from *spo0A* and parental backgrounds R^2 0.48, P-value <0.001, and M9G R^2 0.43, P-value <0.001) (Figure 5B). Direct comparisons between AbrB-GFP noise levels at different srRNA levels also revealed significant changes (Figure 5). The noise increase therefore seems correlated to the level of RnaC/S1022. Notably, this relation was also observed for noise measurements in a *spo0A* deletion background, even though mean AbrB-GFP expression was between 1.37 and 2.32 fold (for LB and M9G respectively, μ=1.79) higher in Δ*spo0A* strains. This suggests that RnaC/S1022 has a specific role in noise modulation of AbrB-GFP.

RnaC/S1022 has no indirect effect on the abrB promoter and is expressed homogeneously

After observing that RnaC/S1022 specifically increases AbrB-GFP expression noise, we aimed to elucidate the origin of this AbrB-GFP noise. Two possibilities for noise generation by an srRNA are conceivable. Firstly RnaC/S1022 could have an additional indirect effect on *abrB* expression, leading to noisy expression from the *abrB* promoter and subsequent propagation of this noise to the AbrB protein level. Secondly, RnaC/S1022 may itself be expressed either in bimodal fashion or with high noise.

To study the distribution of the *abrB* promoter, we integrated the pBaSysBioII plasmid (35) directly behind the Spo0A binding site in the promoter region of *abrB* (36), resulting in a single-copy promoter fusion at the native genomic locus (P_{abrB} ; -41bp of the *abrB* start codon). This location was selected to include the effect of AbrB autorepression and Spo0A(-P) repression, while excluding RnaC/S1022 regulation. We observed no bimodal or particularly noisy expression of this *abrB* promoter fusion, showing that transcription from the *abrB* promoter is homogeneous in the exponential phase (Figure 5C). Of note, bimodal or noisy expression of P_{abrB} would have been surprising since transcription of *abrB* is autorepressed and it is generally found that this NAR reduces the noise of promoter expression (37, 38). Since we observed only a slight increase in *abrB* promoter noise specific to RnaC/S1022 (Figure 5C), the hypothesis that AbrB-GFP noise promotion originates from an additional effect of RnaC/S1022 on the *abrB* promoter can be rejected.

A second possibility of noise promotion by RnaC/S1022 is that it is itself expressed with large noise. In this case, large cell-to-cell variation in srRNA levels would only lead to regulation in cells that have above-threshold srRNA levels, and this could generate the variation in AbrB-GFP levels. We tested this by FC analysis of the integrative RnaC/S1022 promoter fusion ($P_{RnaC/S1022}$; Figure 4) and found this promoter fusion to be homogenously expressed

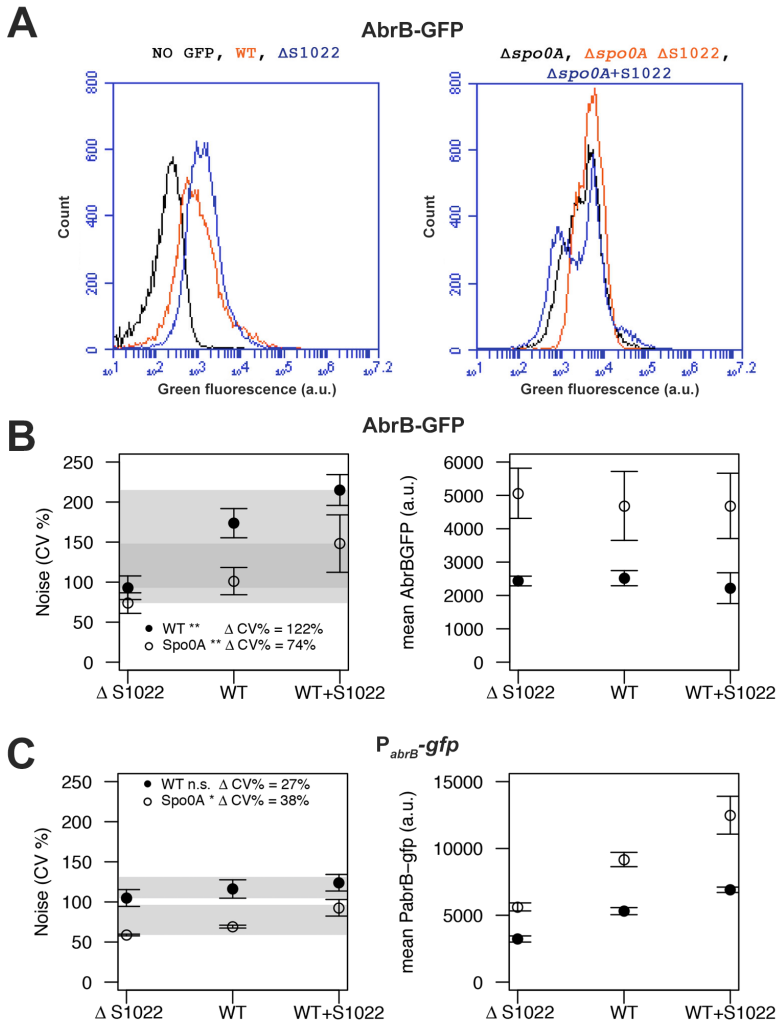

Figure 5. RnaC/S1022 induces protein expression noise of AbrB-GFP.
A) Representative FC data for the genomic AbrB-GFP translational fusion strains grown on M9S. The left panel shows histograms for, from left to right 168^{trp+} (auto-fluorescence), parental strain with AbrB-GFP, and ΔRnaC/S1022 with AbrB-GFP. The right panel shows data in the Δ*spo0A* background for three levels of RnaC/S1022. Please note the increase in the width of the distribution with increasing RnaC/S1022 levels. B) Quantification of AbrB-GFP noise (left panel) and mean expression (right panel) data from three independent M9G experiments. Shaded areas indicate the noise increase (CV%) from 0 to 2 srRNA copies for the parental and Δ*spo0A* background. Significance of statistical comparisons of 0 to 2 srRNA copies for both backgrounds are indicated with asterisks in the legend (* p-value <0.05; ** p-value <0.01; ANOVA with Tukey HSD test. Error bars represent the standard deviation. C) Quantification of P_{abrB}-*gfp* noise (left panel) and mean expression (right panel) data from three independent M9G experiments. Significance of statistical comparisons of 0 to 2 srRNA copies for both backgrounds are indicated with asterisks in the legend (* p-value <0.05; n.s. means not significant; ANOVA with Tukey HSD test. Error bars represent the standard deviation.

with a tight distribution of GFP levels (CV% of 64% for the M9G condition; Figure 4D). As a control for SigD activity we employed the SigD-dependent promoter fusion P_{hag}, and found that this promoter was also expressed with comparable low noise levels (CV% of 62% for the M9G condition; Figure 4E). Notably, this P_{hag} distribution seems to have a low-expression skewed tail, suggesting that there is a small fraction of cells that have very low P_{hag} activity. Previously, a *hag* promoter fusion containing the same region, but integrated in the *amyE* locus, was tested in two other *B. subtilis* strains (PY79 and 3610) and was reported to be bistably expressed in the exponential growth phase (39). However, the latter study did not present data on the *B. subtilis* 168 strain. Besides this observation, we argued that the relatively low expression of $P_{RnaC/S1022}$ could result in threshold-level regulation where the srRNA is only involved in regulating *abrB* in cells with above-threshold levels of RnaC/S1022. However, this is not consistent with the observation of further increased noise levels in cells with two genomic copies of RnaC/S1022 (Figure 5B). We therefore consider the possibility of AbrB noise promotion via heterogeneous expression of RnaC/S1022 highly unlikely.

srRNA-induced protein expression noise is consistent with mathematical models of srRNA regulation

Since the experimental data presented above pointed to a direct role of the RnaC/S1022 srRNA in AbrB protein noise promotion, we wondered whether this possibility is consistent with mathematical models of srRNA regulation. To verify this, we considered a simple model of RNA regulation with two independently transcribed RNA species (srRNA and mRNA) (40, 41, 42). In this model, these molecules are synthesized with constant transcription rates α_s and α_m, respectively. Translation of mRNA into protein *Q*, and the degradation of srRNA, mRNA and protein molecules were modeled as linear processes that occur with rates δ, β_s, β_m, and γ, respectively. The srRNA-mRNA duplex formation was assumed to be an irreversible second-order process that occurs with a rate κ. In the model, molecules in the srRNA-mRNA duplex were removed from the dynamical system. A summary of all reactions and the master equation used in the model can be found in Figure 6.

We first implemented model parameters used in an earlier srRNA modeling study by Jia et al. (42) (Set I; Figure 6A and D). Of note, these parameters were essentially the same as those of Levine et al. (40). In all cases the srRNA transcription rate (α_s) was a free variable to capture the effect of 0, 1, or 2 genomic copies of RnaC/S1022. In addition, for each set of parameters we included two possible α_m values to model the effect in the Spo0A deletion strain where the *abrB* transcription rate (α_m) is approximately two-fold higher than in the parental strain (as determined with P_{abrB}-*gfp*). Varying extrinsic noise in the *abrB* transcription rate had no effect on the general modeling outcome (Supplementary figure 3) and the intermediate α_m CV% level of 40% was selected for plots in the main text. After running the model with parameters from Set I, we observed that model-predicted protein noise strongly increased with increasing α_s. This trend of increasing protein noise with increasing srRNA transcription rates was similar to what we observed for the genomic AbrB-GFP fusion (Figure 5A and B). Importantly, doubling α_m (two-fold higher mRNA transcription rate) resulted in a more gradual noise increase with increasing α_s, just as was observed in the case of Δ*spo0A* with the AbrB-GFP fusion.

We next sought to determine the effect of changing modeling parameters on the modeling outcome, because the selected mRNA half-life of ~35 min (β_m 0.02) in parameter Set I would only be relevant for a subset of mRNA molecules as shown experimentally by Hambraeus et al. (43) (with a relation between these of mean lifetime from Figure 6A * ln 2 = half-life). We therefore constructed a second set of modeling parameters (Set II), which gave the mRNA and srRNA species a half-life of ~3.5 min (β_m and β_s 0.20) while keeping protein half-life at ~35 min. In addition, α_m was increased from 2 transcripts per minute to 4 per minute, and δ was

doubled to 2 synthesized proteins per minute. Although the maximum noise level from these Set II simulations was markedly different, it again clearly showed the trend of increasing protein noise with increasing srRNA transcription rates. We can therefore conclude that the modeling results robustly support the idea that srRNA regulation can generate noise at the protein level. Altogether, our experimental data and the modeling approach are consistent with the view that RnaC/S1022 is an intrinsic noise generator for AbrB-GFP at the post-transcriptional level.

A

Parameter	Value [1/min] Set 1	Set 2
α_s	free	free
β_s	0.02	0.20
α_m	2.00, 4.00	4.00, 8.00
β_m	0.02	0.20
δ	1.00	2.00
γ	0.02	0.02
κ	0.10	0.10

B

$$\emptyset \xrightarrow{\alpha_s} s \qquad s \xrightarrow{\beta_s} \emptyset$$
$$\emptyset \xrightarrow{\alpha_m} m \qquad m \xrightarrow{\beta_m} \emptyset$$
$$m \xrightarrow{\delta} m+q \qquad q \xrightarrow{\gamma} \emptyset$$
$$s+m \xrightarrow{\kappa} \emptyset$$

C

$$\begin{aligned}\frac{dP}{dt}(s,m,q) \;=\; & \alpha_s\,[P(s-1,m,q) - P(s,m,q)] \\ & + \alpha_m\,[P(s,m-1,q) - P(s,m,q)] \\ & + \gamma\, m\,[P(s,m,q-1) - P(s,m,q)] \\ & + \beta_s\,[(s+1)\,P(s+1,m,q) - s\,P(s,m,q)] \\ & + \beta_m\,[(m+1)\,P(s,m+1,q) - m\,P(s,m,q)] \\ & + \delta\,[(q+1)\,P(s,m,q+1) - q\,P(s,m,q)] \\ & + \kappa\,[(s+1)\,(m+1)\,P(s+1,m+1,q) - s\,m\,P(s,m,q)]\end{aligned}$$

D

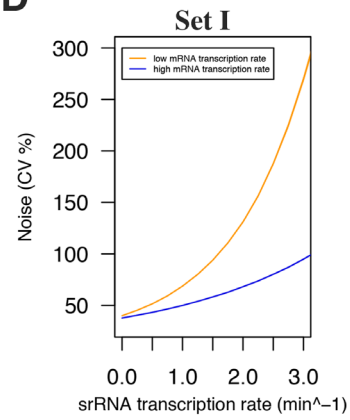

E

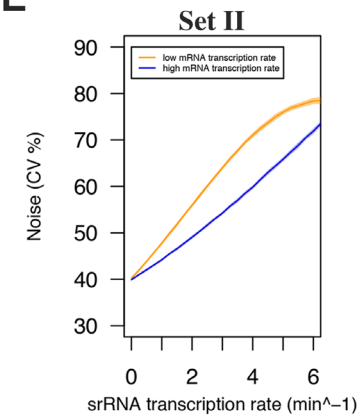

Figure 6. srRNA regulation increases protein expression noise in a stochastic simulation model.
A) Noise-generating dynamics of srRNA regulation were simulated in a stochastic simulation model for two sets of parameters with two mRNA transcription rates and the srRNA transcription rate as a free parameter. B) Reactions considered in the model. C) Master equation used for the model. D) Modeling outcome for parameter Set I. E) Modeling outcome for parameter Set II. Note that modeling with both parameter sets predicts increased protein expression noise with increased srRNA transcription rates. In both cases this effect is buffered by a higher mRNA transcription rate as was observed in Figure 5B for the Δ*spo0A* background.

RnaC/S1022-induced AbrB expression noise generates diversity in growth speeds in the exponential phase

After defining the experimental and theoretical framework for noise promotion by the RnaC/S1022 srRNA, we wondered what the physiological relevance of this regulation might be. Since we and others (Figure 1A; (22)) have reported an effect of AbrB levels on the growth of *B. subtilis*, a growth-related function seemed obvious. Testing the effect of AbrB heterogeneity on growth requires the tracking of cells with low and high AbrB-GFP levels over time. To do this, we performed a live imaging experiment with the Δ*spo0A* AbrB-GFP strain either containing zero srRNA copies (combined with ΔRnaC/S1022) or two genomic copies (combined with pRMC+S1022::*amyE*). The Δ*spo0A* background was used to elevate AbrB-GFP levels and thereby to facilitate fluorescence measurements. Cells were pre-cultured in M9G as was done for the FC measurements and applied to agarose pads (OD_{600} ~0.15) essentially as was described by Piersma et al. (44). From these experiments, and consistent with FC data in Figure 5, it was apparent that there was a larger variation in AbrB-GFP levels in the strain with two genomic RnaC/S1022 copies, compared to the strain lacking RnaC/S1022 (Figure 7B; Supplementary video). In addition, this variation in AbrB-GFP levels was correlated to the variation in growth rates (quantified as the specific cell length increase) observed during the first 20 min of each live imaging run (Figure 7A). We excluded that this growth rate difference was solely dependent on the position on, or quality of, the slide but rather linked to the level of AbrB-GFP (Figure 7C; Supplementary Video).

Notably, in the two example cells from Figure 7C (Supplementary video) AbrB-GFP levels gradually increase in the cell with a low start level (i.e. high level of srRNA repression), which would be consistent with a gradual reduction in RnaC/S1022 expression on this solid agarose medium (Supplementary Figure 2). However, our experimental setting determines the effect of AbrB-GFP on growth before this reduction in RnaC/S1022 becomes relevant (e.g. the first 5 pictures, or 20 min) (Figure 7A). Beyond this, the increase in AbrB-GFP levels observed later (>150 min) in the live imaging experiment seems coupled to a concomitant increase in growth rate (Supplementary Figure 2). This is again consistent with the positive relation of AbrB-GFP levels with growth rate. Interestingly, while we observed a few cells switching their AbrB-GFP expression state from high to low the AbrB-GFP levels were generally stable throughout a cell's lineage. Combined, these analyses show that the RnaC/S1022-induced heterogeneity in the AbrB-GFP expression levels generates diversity in growth rates within the exponential phase of growth.

Discussion

In this study we show that *B. subtilis* employs the RnaC/S1022 srRNA to post-transcriptionally regulate AbrB and that this regulation results in increased heterogeneity in growth rates during the exponential phase of growth. RnaC/S1022 is the third srRNA in *B. subtilis* for which a direct target has been reported and this study reveals the value of evolutionary target predictions to identify true srRNA targets for this species.

The observed growth rate heterogeneity induced by RnaC/S1022 is conceivably of physiological relevance since slowly growing bacterial cells are generally less susceptible to antibiotics and other environmental insults than fast growing cells (45, 46, 47). Specifically, it was noted for *hip* strains of *E. coli* that slowly growing cells within a population will develop into persister cells when challenged with ampicillin (17). Notably, in this system, the initial heterogeneity in growth rates was reported to be dependent on the HipAB toxin-antitoxin module (48). Analogously, it is conceivable that a *B. subtilis* toxin-antitoxin module under negative AbrB control could be responsible for the heterogeneity observed in the present study.

Another perhaps more likely possibility is that low AbrB levels cause the premature activation of transition- or stationary phase genes, thereby slowing down growth and causing premature stationary phase entry. AbrB has also been implicated in the activation of some genes under CCR (22, 23). However, the increased growth rate in cells with higher AbrB levels cannot be explained by CCR since this is also observed during growth with excess glucose (this study; (22)), when CCR is active and AbrB has no activating role. Since the RnaC/S1022 regulation of AbrB reported here is specifically linked to increasing AbrB noise, this can explain the initially observed growth phenotype of ΔRnaC/S1022. Specifically, the absence of RnaC/S1022 will reduce the number of cells expressing AbrB at a low level. Growth of the ΔRnaC/S1022 population will therefore be more homogeneous and, when inspected as an average, the

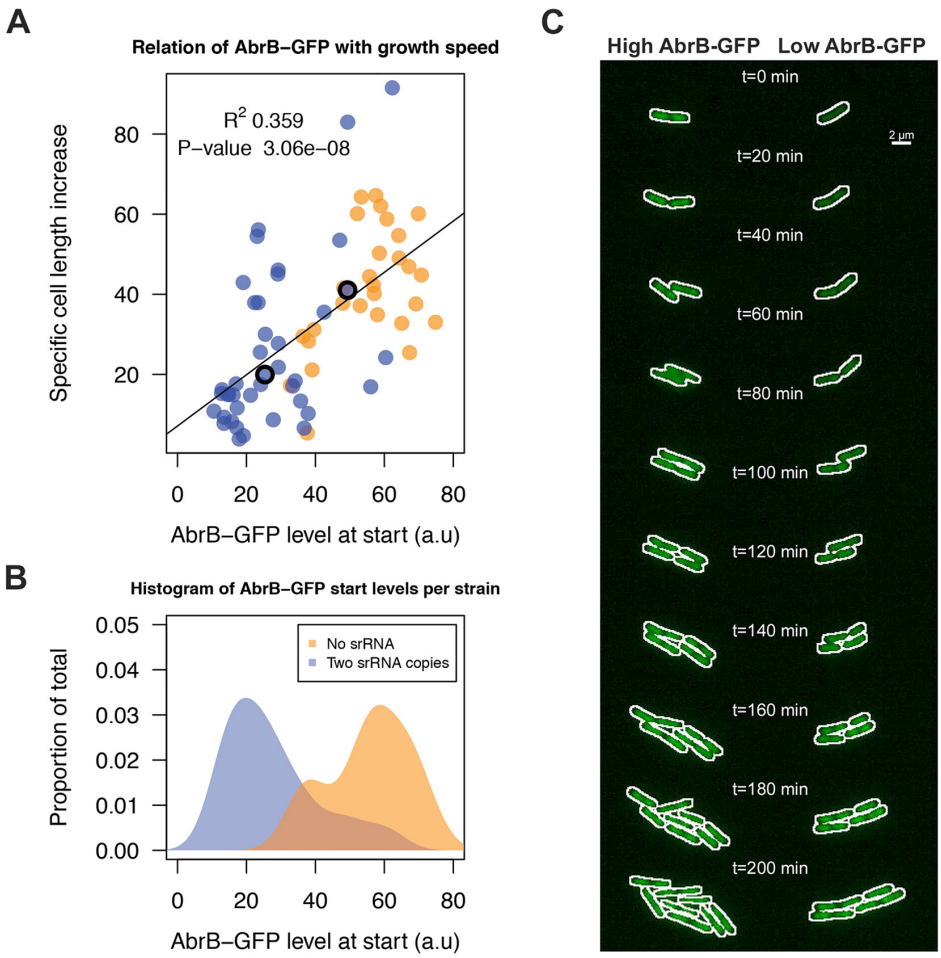

Figure 7. RnaC/S1022-induced variation in AbrB-GFP levels leads to heterogeneity in growth rates.
A) Tracing of growth and AbrB-GFP levels of 71 individual micro-colonies from Δ*spo0A* AbrB-GFP strains with either zero or two genomic copies of RnaC/S1022. Data originates from three independent experiments. Cell growth is expressed as the cell length (Feret's diameter) increase per h as determined in the first 20 min after being spotted on agarose slides. The plotted AbrB-GFP level is the average of fluorescence in the first and second picture. B) Distribution of AbrB-GFP start levels for both strains. Note that two genomic RnaC/S1022 copies lead to a wider distribution of AbrB-GFP levels. C) Montage of the two adjacent dividing cells from Supplementary Movie 1. The white outline marks the contours of the cell. The positions of these cells in panel A are marked with an **O**. Individual cells were cropped for illustration purposes only.

population will enter stationary phase later than the parental strain. Beyond the mechanism of AbrB-mediated growth regulation, we show that noisy regulation of a growth regulator can also cause heterogeneity in growth rates. This suggests that the AbrB noise level has been fine-tuned in evolution, possibly as a bet-hedging strategy to deal with environmental insults.

Two other questions addressed by this study are the origin of AbrB expression noise, and the likely reason why this noise is generated at the post-transcriptional level. The origin of AbrB expression noise via triggering of *abrB* mRNA degradation and/or inhibition of *abrB* translation fits the definition of an intrinsic noise source where the absence of RnaC/S1022 reduces the number of sources for intrinsic noise by one, and therefore results in lower protein expression noise. This specific noise-generating capacity of srRNA regulation might be due to the specific kinetics of the RnaC/S1022- *abrB* mRNA interaction. It is currently unclear whether this feature of srRNA-mediated regulation can be extended to other srRNA-mRNA pairs. Specifically, subtle consequences of srRNA regulation, such as noise generation, may have been overlooked in previous studies due to the use of plasmid-encoded translational fusions with fluorescent proteins expressed from strong non-native promoters as reporters. We therefore expressed all RnaC/S1022 and AbrB-GFP constructs from their native genomic location, from their native promoters, and assayed the effects in the relevant growth phase.

NAR of AbrB seems to be the answer to the second question why noise is generated post-transcriptionally and not at the promoter level. AbrB's NAR is important for its functioning in the stationary phase sporulation network (26, 27) and is therefore likely a constraint for evolutionary optimization of AbrB expression in the exponential phase, which is the growth phase addressed in this study. In turn, NAR is a clear constraint on noise generation since it is generally believed to dampen noise (37, 38). Consistent with this view, we observed only a slight increase in P_{abrB} promoter noise upon increasing AbrB protein noise, suggesting that AbrB NAR is responsible for minimizing promoter noise. Besides reducing noise, NAR has been implicated in decreasing the response time of a genetic circuit, linearizing the dose response of an inducer, and increasing the input dynamic range of a transcriptional circuit (19). Individually, and in combination, these mechanistic aspects of NAR could explain why NAR is such a widespread phenomenon in transcriptional regulation. Besides this, the idea that AbrB and AbrB NAR are more widely conserved than RnaC/S1022 would be in line with the idea that AbrB expression in *B. subtilis* 168 has become fine-tuned by an additional regulator which has evolved later in time. Lastly, on a more general note, the inconsistency between the *abrB* promoter and AbrB protein noise measurements make it clear that it is premature to draw conclusions about homogeneity or heterogeneity of protein expression when only data is gathered at the promoter level, especially for genes under a NAR regime.

In conclusion, we have identified a novel direct srRNA target in the important *B. subtilis* transcriptional regulator *abrB*. Specifically, we provide functionally and physiologically relevant explanations for the evolution of the noise-generation aspects of this regulation in generating heterogeneity in growth rates. This noise is induced at the post-transcriptional level due to AbrB NAR. Based on our present observations, we hypothesize that the resulting subpopulations of fast- and slow-growing *B. subtilis* cells reflect an evolutionary conserved bet-hedging strategy for enhanced survival of unfavorable conditions.

Materials and Methods

Bacterial strain construction

E. coli and *B. subtilis* strains and plasmids used in this study are listed in Supplementary Table II and oligonucleotides in Supplementary Table III. *E. coli* TG1 was used for all cloning procedures. All *B. subtilis* strains were based on the *trpC2*-proficient parental strain 168. *B.*

subtilis transformations were performed as described previously (49). The isogenic RnaC/S1022 mutant was constructed according to the method described by Tanaka et al. (50). pRMC was derived from pXTC (51) by Circular Polymerase Extension Cloning (CPEC) (52) with primers ORM0054 and ORM0055 using pXTC as PCR template and ORM0056 to circularize this PCR fragment in the final CPEC reaction. In this manner, the xylose-inducible promoter of pXTC was replaced with the *Asc*I Ligation Independent Cloning (LIC; (53)) site from pMUTIN-GFP (54). As a consequence, pRMC carries a cassette that can be integrated into the *amyE* locus via double cross-over recombination, allowing ectopic expression of genes in single copy from their native promoter. RnaC/S1022 was cloned in pRMC under control of its native promoter as identified by Schmalisch et al. (28), and the subsequent integration of RnaC/S1022 into the *amyE* locus via double cross-over recombination was confirmed by verifying the absence of α-amylase activity on starch plates. The LIC plasmid pRM3+P_{wt} RnaC/S1022, which is a derivative of plasmid pHB201 (55), was used to express RnaC/S1022 under control of its native promoter. The RnaC/S1022, *hag* and *abrB* promoter *gfp* fusions were constructed at the native chromosomal locus by single cross-over integration of the pBSBII plasmid (35). A minimum of three clones were checked to exclude possible multi-copy integration of the plasmid.

Media and growth conditions

Lysogeny Broth (LB) consisted of 1% tryptone, 0.5% yeast extract and 1% NaCl, pH 7.4. M9 medium supplemented with either 0.3% glucose (M9G) or 0.3% sucrose (M9S) was freshly prepared from separate stock solutions on the day of the experiment as previously described (9). For live cell imaging experiments, the M9 medium was filtered through a 0.2 mm Whatman™ filter (GE Healthcare). Strains were grown with vigorous agitation at 37 °C in either Luria LB or M9 medium using an orbital shaker or a Biotek Synergy 2 plate reader at maximal shaking. Growth was recorded by optical density readings at 600 nm (OD_{600}). When required, media for *E. coli* were supplemented with ampicillin (100 mg ml^{-1}) or chloramphenicol (10 mg ml^{-1}); media for *B. subtilis* were supplemented with phleomycin (4 mg ml^{-1}), kanamycin (20 mg ml^{-1}), tetracyclin (5 mg ml^{-1}), chloramphenicol (10 mg ml^{-1}), erythromycin (2 g ml^{-1}), and spectinomycin (100 mg ml^{-1}) or combinations thereof.

Evolutionary conservation analysis of RnaC/S1022 targets

In order to find predicted targets co-conserved with RnaC/S1022, we used the 62 *Bacillus* genomes available in Genbank (as of January 31, 2013). On each of these genomes a BLAST search (Blastn v2.2.26 with default parameters) was conducted with the *B. subtilis* 168 RnaC/S1022 sequence as identified in Nicolas et al. (9). Genomes where a homologue of RnaC/S1022 (E-value < 0.001) was found were then subjected to TargetRNA_v1 search with extended settings around the 5'UTR (-75 bp; +50 bp around the start codon and additional command line arguments "-z 250 -y 2 -l 6") using as query the sequence of the first high-scoring-pair of the first BLAST hit in that particular genome. A bidirectional best hit criterion (based on Blastp v2.2.26 with default parameters and E-value cut-off 0.001) was used to compare the predicted targets in each genome with the predicted targets in the reference *B. subtilis* 168 genome (Genbank: AL009126-3). The data was tabulated and subsetted for *B. subtilis* 168 genes predicted for RnaC/S1022 in 8 or more genomes.

The *Bacillaceae* phylogenetic tree was computed based on an alignment of the *rpoB* gene BLAST result from the same set of genomes mentioned above. *RpoB* was reported to be a better determinant of evolutionary relatedness for *Bacillus* species than 16S rRNA (56).

Western blot, RNA isolation and Northern blot

Cultures grown on LB, M9G, or M9S were sampled in mid-exponential growth phase (OD_{600} 0.4 – 0.6) and were directly harvested in killing buffer and processed as previously described (9). Northern blot analysis was carried out as described previously (57). The digoxigenin-labeled RNA probe was synthesized by *in vitro* transcription with T7 RNA polymerase and an *abrB* specific PCR product as template. 5 µg of total RNA per lane was separated on 1.2% agarose gels. Chemiluminescence signals were detected using a ChemoCam Imager (Intas Science Image Instruments GmbH, Göttingen, Germany).

Western blot analysis was performed as described (58) using crude whole cell lysates. To prepare lysates, cell pellets were resuspended in LDS-sample buffer with reducing agent (Life technologies), and disrupted with glass beads in a bead beater (3 x 30 sec at 6500 rpm with 30 sec intermittences). Before loading on Novex nuPAGE 10% Bis-Tris gels (Life technologies), samples were boiled for 10 min and centrifuged to pellet the glass beads and cell debris. Equal OD units were loaded on gel and the intensity of the AbrB band was corrected with the intensity for the unrelated BdbD control.

Computation of promoter activity

Promoter activity was monitored every 10 min from cells grown in 96-well plates in a Biotek® Synergy 2 plate reader. Promoter activity was computed by subtracting the fluorescence of the previous time-point from that of the measured time-point (as in Botella et al. (35)). Moving average filtering (*filter* function in R with filter=rep(1/5, 5) was applied for smoothing of the promoter activity plots.

Flow cytometry and noise measurements

Cultures grown on LB, M9G, or M9S were sampled in mid-exponential growth phase OD_{600} 0.4 – 0.5 and were directly analyzed in a Accuri C6 flow cytometer. The number of recorded events within a gate set with growth medium was 15,000. The coefficient of variation (i.e. relative standard deviation) (CV%; standard deviation / mean * 100%) was used as a measure of the width of the distribution, or protein/promoter expression noise.

Live imaging

Live imaging analysis was conducted on aerated agarose cover slips as described previously (44). Segmentation, calculation of Feret diameter, and auto-fluorescence correction for every microcolony were also performed as described by Piersma et al. (44). Subsequent computations and plotting was done with R. The specific cell length (Feret diameter) increase per hour was computed as follows: ((cumulative Feret diameter at $t_{20\,min}$ / number of cells at $t_{0\,min}$) – (cumulative Feret diameter at $t_{0\,min}$ / number of cells at $t_{0\,min}$)) / (($t_{20\,min}$ – $t_{0\,min}$) / 60 min).

Modeling noise

Noise promoting dynamics by srRNA regulation was modeled in a stochastic simulation model (40, 41, 42). The considered reactions, employed parameters, and the master equation are listed in Figure 6. The master equation was numerically integrated by employing an in-house developed implementation of the Gillespie algorithm (59) for each combination of model parameters. The stochastic simulations were started without any molecules and were run until a quasi-stationary state was reached. To capture the inherent stochasticity of the model we performed, for each set of model parameters, 50 x 10,000 simulation replicates (i.e. 500,000 in total). This can be interpreted as 50 experiments involving 10,000 cells each. Mean, standard deviation, and the

median was computed for every molecular species in the population of 10,000 cells.

Acknowledgements

The authors would like to thank Brian Tjaden for the TargetRNA_v1 source code and Peter Lewis for kindly providing the AbrB-GFP fusion.

Supplementary Material (available on request; email rubenmars@gmail.com)

Figure S1-S3
Supplementary Table I-III
Supplementary Video

Legends and selected Supplementary Figure

Supplementary Figure 1. Competence is decreased in a RnaC/S1022 mutant
Competence was assayed by transformation with plasmid pHB201. Error bars represent the standard deviation between three replicate experiments.

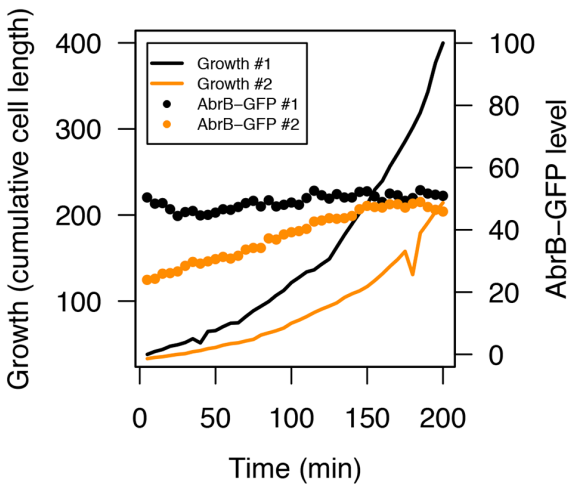

Supplementary Figure 2. Growth and AbrB-GFP levels of colonies from Figure 7C and Supplementary Video 1.
Cell growth is expressed as the cumulative cell length (Feret's diameter). Cell #1 with a higher initial AbrB-GFP level grows faster than cell #2 with a lower initial AbrB-GFP level.

Supplementary Figure 3. Modeling outcome for both sets of parameters at variable extrinsic noise levels
Modeling outcome as described in Figure 6 for all five considered intrinsic noise levels obtained with parameter Sets I and II. Different intrinsic noise levels are marked with differently colored symbols.

References

1. Buescher,J.M., Liebermeister,W., Jules,M., Uhr,M., Muntel,J., Botella,E., Hessling,B., Kleijn,R.J., Le Chat,L., Lecointe,F., et al. (2012) Global network reorganization during dynamic adaptations of bacillus subtilis metabolism. *Science,* **335,** 1099-1103.
2. Beisel,C.L. and Storz,G. (2010) Base pairing small RNAs and their roles in global regulatory networks. *FEMS Microbiol. Rev.,* **34,** 866-882.
3. Storz,G., Vogel,J. and Wassarman,K.M. (2011) Regulation by small RNAs in bacteria: Expanding frontiers. *Mol. Cell,* **43,** 880-891.
4. Aiba,H. (2007) Mechanism of RNA silencing by hfq-binding small RNAs. *Curr. Opin. Microbiol.,* **10,** 134-139.
5. Gaballa,A., Antelmann,H., Aguilar,C., Khakh,S.K., Song,K.B., Smaldone,G.T. and Helmann,J.D. (2008) The bacillus subtilis iron-sparing response is mediated by a fur-regulated small RNA and three small, basic proteins. *Proc. Natl. Acad. Sci. U. S. A.,* **105,** 11927-11932.
6. Heidrich,N., Chinali,A., Gerth,U. and Brantl,S. (2006) The small untranslated RNA SR1 from the bacillus subtilis genome is involved in the regulation of arginine catabolism. *Mol. Microbiol.,* **62,** 520-536.
7. Smaldone,G.T., Revelles,O., Gaballa,A., Sauer,U., Antelmann,H. and Helmann,J.D. (2012) A global investigation of the bacillus subtilis iron-sparing response identifies major changes in metabolism. *J. Bacteriol.,* **194,** 2594-2605.
8. Irnov,I., Sharma,C.M., Vogel,J. and Winkler,W.C. (2010) Identification of regulatory RNAs in bacillus subtilis. *Nucleic Acids Res.,* **38,** 6637-6651.
9. Nicolas,P., Mader,U., Dervyn,E., Rochat,T., Leduc,A., Pigeonneau,N., Bidnenko,E., Marchadier,E., Hoebeke,M., Aymerich,S., et al. (2012) Condition-dependent transcriptome reveals high-level regulatory architecture in bacillus subtilis. *Science,* **335,** 1103-1106.
10. Raj,A. and van Oudenaarden,A. (2008) Nature, nurture, or chance: Stochastic gene expression and its consequences. *Cell,* **135,** 216-226.
11. Losick,R. and Desplan,C. (2008) Stochasticity and cell fate. *Science,* **320,** 65-68.
12. Maamar,H., Raj,A. and Dubnau,D. (2007) Noise in gene expression determines cell fate in bacillus subtilis. *Science,* **317,** 526-529.
13. Chastanet,A., Vitkup,D., Yuan,G.C., Norman,T.M., Liu,J.S. and Losick,R.M. (2010) Broadly heterogeneous activation of the master regulator for sporulation in bacillus subtilis. *Proc. Natl. Acad. Sci. U. S. A.,* **107,** 8486-8491.
14. Veening,J.W., Smits,W.K. and Kuipers,O.P. (2008) Bistability, epigenetics, and bet-hedging in bacteria. *Annu. Rev. Microbiol.,* **62,** 193-210.
15. Elowitz,M.B., Levine,A.J., Siggia,E.D. and Swain,P.S. (2002) Stochastic gene expression in a single cell. *Science,* **297,** 1183-1186.
16. Paulsson,J. (2004) Summing up the noise in gene networks. *Nature,* **427,** 415-418.
17. Balaban,N.Q., Merrin,J., Chait,R., Kowalik,L. and Leibler,S. (2004) Bacterial persistence as a phenotypic switch. *Science,* **305,** 1622-1625.
18. Eldar,A. and Elowitz,M.B. (2010) Functional roles for noise in genetic circuits. *Nature,* **467,** 167-173.
19. Madar,D., Dekel,E., Bren,A. and Alon,U. (2011) Negative auto-regulation increases the input dynamic-range of the arabinose system of escherichia coli. *BMC Syst. Biol.,* **5,** 111-0509-5-111.
20. Saile,E. and Koehler,T.M. (2002) Control of anthrax toxin gene expression by the transition state regulator abrB. *J. Bacteriol.,* **184,** 370-380.
21. Glaser,P., Frangeul,L., Buchrieser,C., Rusniok,C., Amend,A., Baquero,F., Berche,P., Bloecker,H., Brandt,P., Chakraborty,T., et al. (2001) Comparative genomics of listeria species. *Science,* **294,** 849-852.
22. Fisher,S.H., Strauch,M.A., Atkinson,M.R. and Wray,L.V.,Jr. (1994) Modulation of bacillus subtilis catabolite repression by transition state regulatory protein AbrB. *J. Bacteriol.,* **176,** 1903-1912.
23. Mader,U., Schmeisky,A.G., Florez,L.A. and Stulke,J. (2012) SubtiWiki--a comprehensive community resource for the model organism bacillus subtilis. *Nucleic Acids Res.,* **40,** D1278-87.
24. Chumsakul,O., Takahashi,H., Oshima,T., Hishimoto,T., Kanaya,S., Ogasawara,N. and Ishikawa,S. (2011) Genome-wide binding profiles of the bacillus subtilis transition state regulator AbrB and its homolog abh reveals their interactive role in transcriptional regulation. *Nucleic Acids Res.,* **39,** 414-428.
25. Bobay,B.G., Benson,L., Naylor,S., Feeney,B., Clark,A.C., Goshe,M.B., Strauch,M.A., Thompson,R. and Cavanagh,J. (2004) Evaluation of the DNA binding tendencies of the transition state regulator AbrB. *Biochemistry,* **43,** 16106-16118.
26. Banse,A.V., Chastanet,A., Rahn-Lee,L., Hobbs,E.C. and Losick,R. (2008) Parallel pathways of repression and antirepression governing the transition to stationary phase in bacillus subtilis. *Proc. Natl. Acad. Sci. U. S. A.,* **105,** 15547-15552.
27. Schultz,D., Wolynes,P.G., Ben Jacob,E. and Onuchic,J.N. (2009) Deciding fate in adverse times: Sporulation and competence in bacillus subtilis. *Proc. Natl. Acad. Sci. U. S. A.,* **106,** 21027-21034.
28. Schmalisch,M., Maiques,E., Nikolov,L., Camp,A.H., Chevreux,B., Muffler,A., Rodriguez,S., Perkins,J. and Losick,R.

(2010) Small genes under sporulation control in the bacillus subtilis genome. *J. Bacteriol.,* **192,** 5402-5412.
29. Will,S., Joshi,T., Hofacker,I.L., Stadler,P.F. and Backofen,R. (2012) LocARNA-P: Accurate boundary prediction and improved detection of structural RNAs. *RNA,* **18,** 900-914.
30. Nicholson,W.L. (2012) Increased competitive fitness of bacillus subtilis under nonsporulating conditions via inactivation of pleiotropic regulators AlsR, SigD, and SigW. *Appl. Environ. Microbiol.,* **78,** 3500-3503.
31. Tjaden,B. (2008) TargetRNA: A tool for predicting targets of small RNA action in bacteria. *Nucleic Acids Res.,* **36,** W109-13.
32. Xu,K., Clark,D. and Strauch,M.A. (1996) Analysis of abrB mutations, mutant proteins, and why abrB does not utilize a perfect consensus in the -35 region of its sigma A promoter. *J. Biol. Chem.,* **271,** 2621-2626.
33. Hahn,J., Roggiani,M. and Dubnau,D. (1995) The major role of Spo0A in genetic competence is to downregulate abrB, an essential competence gene. *J. Bacteriol.,* **177,** 3601-3605.
34. Peer,A. and Margalit,H. (2011) Accessibility and evolutionary conservation mark bacterial small-rna target-binding regions. *J. Bacteriol.,* **193,** 1690-1701.
35. Botella,E., Fogg,M., Jules,M., Piersma,S., Doherty,G., Hansen,A., Denham,E.L., Le Chat,L., Veiga,P., Bailey,K., et al. (2010) pBaSysBioII: An integrative plasmid generating gfp transcriptional fusions for high-throughput analysis of gene expression in bacillus subtilis. *Microbiology,* **156,** 1600-1608.
36. Greene,E.A. and Spiegelman,G.B. (1996) The Spo0A protein of bacillus subtilis inhibits transcription of the abrB gene without preventing binding of the polymerase to the promoter. *J. Biol. Chem.,* **271,** 11455-11461.
37. Becskei,A. and Serrano,L. (2000) Engineering stability in gene networks by autoregulation. *Nature,* **405,** 590-593.
38. Dublanche,Y., Michalodimitrakis,K., Kummerer,N., Foglierini,M. and Serrano,L. (2006) Noise in transcription negative feedback loops: Simulation and experimental analysis. *Mol. Syst. Biol.,* **2,** 41.
39. Kearns,D.B. and Losick,R. (2005) Cell population heterogeneity during growth of bacillus subtilis. *Genes Dev.,* **19,** 3083-3094.
40. Levine,E., Zhang,Z., Kuhlman,T. and Hwa,T. (2007) Quantitative characteristics of gene regulation by small RNA. *PLoS Biol.,* **5,** e229.
41. Arbel-Goren,R., Tal,A., Friedlander,T., Meshner,S., Costantino,N., Court,D.L. and Stavans,J. (2013) Effects of post-transcriptional regulation on phenotypic noise in escherichia coli. *Nucleic Acids Res.,* **41,** 4825-4834.
42. Jia,Y., Liu,W., Li,A., Yang,L. and Zhan,X. (2009) Intrinsic noise in post-transcriptional gene regulation by small non-coding RNA. *Biophys. Chem.,* **143,** 60-69.
43. Hambraeus,G., von Wachenfeldt,C. and Hederstedt,L. (2003) Genome-wide survey of mRNA half-lives in bacillus subtilis identifies extremely stable mRNAs. *Mol. Genet. Genomics,* **269,** 706-714.
44. Piersma,S., Denham,E.L., Drulhe,S., Tonk,R.H., Schwikowski,B. and van Dijl,J.M. (2013) TLM-quant: An open-source pipeline for visualization and quantification of gene expression heterogeneity in growing microbial cells. *PLoS One,* **8,** e68696.
45. Gefen,O. and Balaban,N.Q. (2009) The importance of being persistent: Heterogeneity of bacterial populations under antibiotic stress. *FEMS Microbiol. Rev.,* **33,** 704-717.
46. TUOMANEN,E., COZENS,R., TOSCH,W., ZAK,O. and TOMASZ,A. (1986) The rate of killing of escherichia coli byß-lactam antibiotics is strictly proportional to the rate of bacterial growth. *Journal of General Microbiology,* **132,** 1297-1304.
47. Hecker,M., Pane-Farre,J. and Volker,U. (2007) SigB-dependent general stress response in bacillus subtilis and related gram-positive bacteria. *Annu. Rev. Microbiol.,* **61,** 215-236.
48. Rotem,E., Loinger,A., Ronin,I., Levin-Reisman,I., Gabay,C., Shoresh,N., Biham,O. and Balaban,N.Q. (2010) Regulation of phenotypic variability by a threshold-based mechanism underlies bacterial persistence. *Proc. Natl. Acad. Sci. U. S. A.,* **107,** 12541-12546.
49. Kunst,F. and Rapoport,G. (1995) Salt stress is an environmental signal affecting degradative enzyme synthesis in bacillus subtilis. *J. Bacteriol.,* **177,** 2403-2407.
50. Tanaka,K., Henry,C.S., Zinner,J.F., Jolivet,E., Cohoon,M.P., Xia,F., Bidnenko,V., Ehrlich,S.D., Stevens,R.L. and Noirot,P. (2013) Building the repertoire of dispensable chromosome regions in bacillus subtilis entails major refinement of cognate large-scale metabolic model. *Nucleic Acids Res.,* **41,** 687-699.
51. Darmon,E., Dorenbos,R., Meens,J., Freudl,R., Antelmann,H., Hecker,M., Kuipers,O.P., Bron,S., Quax,W.J., Dubois,J.Y., et al. (2006) A disulfide bond-containing alkaline phosphatase triggers a BdbC-dependent secretion stress response in bacillus subtilis. *Appl. Environ. Microbiol.,* **72,** 6876-6885.
52. Quan,J. and Tian,J. (2009) Circular polymerase extension cloning of complex gene libraries and pathways. *PLoS One,* **4,** e6441.
53. Haun,R.S., Serventi,I.M. and Moss,J. (1992) Rapid, reliable ligation-independent cloning of PCR products using modified plasmid vectors. *BioTechniques,* **13,** 515-518.
54. Doherty,G.P., Fogg,M.J., Wilkinson,A.J. and Lewis,P.J. (2010) Small subunits of RNA polymerase: Localization, levels and implications for core enzyme composition. *Microbiology,* **156,** 3532-3543.

55. Bron,S., Bolhuis,A., Tjalsma,H., Holsappel,S., Venema,G. and van Dijl,J.M. (1998) Protein secretion and possible roles for multiple signal peptidases for precursor processing in bacilli. *J. Biotechnol.,* **64,** 3-13.
56. Ki,J.S., Zhang,W. and Qian,P.Y. (2009) Discovery of marine bacillus species by 16S rRNA and rpoB comparisons and their usefulness for species identification. *J. Microbiol. Methods,* **77,** 48-57.
57. Homuth,G., Masuda,S., Mogk,A., Kobayashi,Y. and Schumann,W. (1997) The dnaK operon of bacillus subtilis is heptacistronic. *J. Bacteriol.,* **179,** 1153-1164.
58. Zweers,J.C., Wiegert,T. and van Dijl,J.M. (2009) Stress-responsive systems set specific limits to the overproduction of membrane proteins in bacillus subtilis. *Appl. Environ. Microbiol.,* **75,** 7356-7364.
59. Gillespie,D.T. (1977) Exact stochastic simulation of coupled chemical reactions. *J. Phys. Chem.,* **81,** 2340-2361.